TR 232

Technical Report 232

THE MEASUREMENT OF HEAT FLOW IN THE GROUND AND THE THEORY OF HEAT FLUX METERS

Peter Schwerdtfeger

November 1970

CORPS OF ENGINEERS, U.S. ARMY
COLD REGIONS RESEARCH AND ENGINEERING LABORATORY
HANOVER, NEW HAMPSHIRE

38

THE MEASUREMENT OF HEAT FLOW IN THE GROUND AND THE THEORY OF HEAT FLUX METERS

Peter Schwerdtfeger

November 1970

DA TASK 4A062112A89401

CORPS OF ENGINEERS, U.S. ARMY
COLD REGIONS RESEARCH AND ENGINEERING LABORATORY
HANOVER, NEW HAMPSHIRE

PREFACE

The experimental and analogue analysis aspects of this work were performed at the Meteorology Department, University of Melbourne, Australia and some of the results were communicated to a meeting of the Australian New Zealand Association for the Advancement of Science in 1967. The numerical aspects were pursued while the author was supported by the Alexander von Humboldt Foundation in 1969 at the Institute of Geophysics and Meteorology, University of Köln, Germany, where a number of discussions with Professor G. Hofmann and the computing assistance of Dr. G. Berz proved to be most valuable. Finally, the results were interpreted and some computations elaborated along lines suggested by Dr. Y. Nakano during the period the author was retained as an Expert by the U.S. Army Cold Regions Research and Engineering Laboratory, Hanover, New Hampshire.

This report was published under DA Task 4A062112A89401.

Manuscript submitted January 1970

CONTENTS

ILLUSTRATIONS

CONTENTS (Cont'd)

ILLUSTRATIONS (Cont'd)

TABLES

THE MEASUREMENT OF HEAT FLOW IN THE GROUND AND THE THEORY OF HEAT FLUX METERS

by

Peter Schwerdtfeger

INTRODUCTION AND REVIEW

The micrometeorological heat balance equation for an impervious, opaque terrestrial surface is:

$$R + G + H + LE = 0 \qquad (1)$$

where the variables represent fluxes in one dimension normal to the surface: R is the net radiation, G the ground heat flow, H the sensible heat transfer in the air and LE the heat associated with evaporation (or condensation) of water. Flows of energy representing a gain for the surface (no matter from which direction) are shown as positive.

Because almost invariably either daily or annual mean values are sought for the various flows of energy, the importance of precise knowledge of the soil heat flow has been almost entirely eliminated. In the absence of any horizontal component, ground heat flow in an impervious dry medium is a completely reversible process. Thus the annual and often the diurnal mean heat flow become very small compared to the mean values of the other terms in eq 1 which emphatically represent nonreversible processes.

The result is that the precise measurement of ground heat flow has come to be one of the micrometeorologist's most neglected skills. There are, however, numerous examples of nonreversible conduction in natural bodies, particularly during the formation of ice covers on water, where almost all the heat of formation is conducted upward through the ice and melting occurs largely at the upper surface. Heat flow measurements are similarly important in translucent media such as ice and snow, where the mean annual conduction must be directed toward the surface because of radiation absorption at depth. With present day interest turning to the study of transfer processes over much shorter periods of time, especially in stands of vegetation where extremes reached during the day can be of the utmost importance, soil heat flow measurements of greatly increased accuracy are called for. One such study has been reported by Ho, Schwerdtfeger and Weller (1968).

Passive heat flow transducers in one form or another are used as sensors of both conducted and radiated heat. In the former application the sensor becomes known as a heat flux (or flow) meter (HFM) and in the latter as a net radiometer. Various types of active sensors, which depend on the generation of a perturbing or in some cases compensating source of heat, also exist. The present study will concern only passive devices, where response is a direct result of the temperature distribution on its sensitive surfaces.

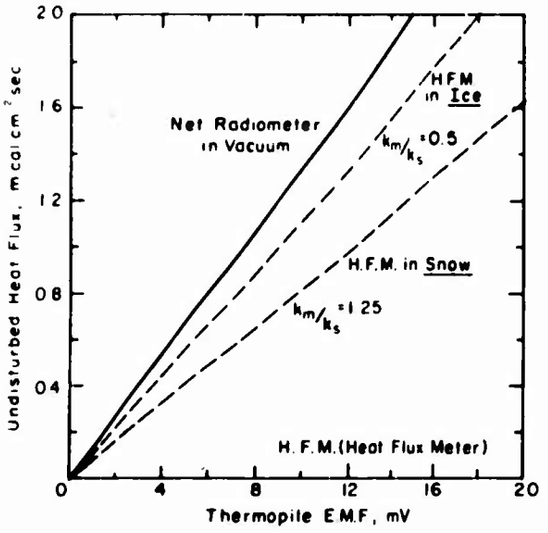

Figure 1. Response of a cylindrical thermopile 4.5 cm in diameter and 1.25 cm thick surrounded by a Perspex annulus of 15 cm outer diameter when temporarily operated as a net radiometer in vacuum and as an HFM in ice and snow of thermal conductivity 5 × 10^{-3} and 2 × 10^{-3} cal cm^{-1} $°C^{-1}$ sec^{-1} respectively. The method of establishing the conductivity ratio k_m/k_s is described on p. 25-29.

It is instructive to take a given heat flow transducer, say a thermopile with two parallel faces, operate it as an HFM to monitor undisturbed and known one-dimensional heat flows in a number of media of differing thermal conductivity, and subsequently convert it to a net radiometer exposed to known radiative conditions. For most thermopile geometries, it quickly becomes evident that only when the sensor is used as a net radiometer can the actual heat flow through it be established relatively easily. If this sensor consists of a thermopile sandwiched between parallel flat plates of known temperature and blackness, the heat flow through it can be calculated if the equilibrium fluxes of radiation incident at the two bounding surfaces are known. The edges, of course, must be radiatively inactive. In contrast to this relatively simple situation, Schwerdtfeger and Weller (1967) have observed that the sensitivity of identical thermopiles used as HFM's in ice and snow depends on the conductivity of the surroundings and may be quite different from the sensitivity of the same sensor operated as a radiometer (Fig. 1). The relationship between HFM's and their equivalent net radiometers will be discussed in greater detail later.

The fact that HFM's of differing conductivity to the surroundings in which they are installed distort the undisturbed heat flow is well known, as the literature survey of Nickerson, Choi and Marcus (1959) indicates. Nickerson and Umur (1960) followed this review, recognizing the lack of quantitative discussion, with a study of a limited number of two- and three-dimensional cases by means of manual digital computation. Some additional two-dimensional work was reported using an analogue technique based on electrically conductive paper and paints. Uncertainty with regard to the resistivity of the painted areas simulating an HFM led to unsatisfactory quantitative results.

Portman (1958) has discussed the results of measurements with a liquid analogue electrical conductivity tank in obtaining data for a single three-dimensional HFM. As Philip (1961) pointed

out subsequently, Portman's suggested functional relationship between HFM geometry and the conductivity ratio is incorrect. Philip showed, with some reservation, how Portman's data actually supported Philip's theoretically derived relation which is strictly applicable to a spheroidal HFM only. In the present work, it will be shown extremely simply that, with some precautions, an equation of the form desired by Philip can reasonably be expected to hold more generally. Testing with new two- and three-dimensional data supports this, although it will be shown that the numerical values suggested by Philip cannot lead to reliable results over the range of HFM geometries suggested. Care must be exercised in the use of Portman's analogue data because of the use of a tank simulating the HFM whose (perturbing) total wall thickness represents 13% of the same tank's thickness. Even though the presence of nonconnected conductors allowed passage of the electric current simulating heat flow normal to the tank faces, the thickness of these was not compensated for in the exterior conducting liquid simulating the HFM surroundings.

All previous analytical work appears to have been directed to HFM's of uniform conductivity which, of course, even the simplest of HFM's equipped with metal cover plates and insulating side walls is not. Furthermore, the geometric and conductive ratios for an HFM which may at first sight appear ideal from purely thermal considerations almost certainly become less favorable when the often unknown factors of thermal contact, not to mention the perturbation of other processes normally occurring simultaneously, are considered. Of paramount importance is the disturbing effect on the soil diffusion of water, the presence of which strongly influences the thermal conductivity and hence HFM sensitivity. Another striking example concerns the undesirable interception of visible radiation by HFM's in translucent or even transparent media such as snow and ice.

There may be good reason therefore, in some applications, to use HFM's that perturb processes other than heat conduction (but which do have an indirect bearing on the temperature distribution) as little as possible, while accepting a distortion of the heat flow in the vicinity of the HFM. Provided that this distortion is known accurately enough, the resultant measurement becomes more reliable. This method appears to be the best approach to heat flux measurements in snow and ice when radiation intensities are high, where Schwerdtfeger and Weller (1967) have used HFM's of low radiative but high conductive cross section. In other cases such as soil, where the maintenance of the undisturbed pattern of water diffusion is important, it is probable that most of the ideal thermal characteristics can be kept for an HFM even if holes are drilled through to allow the relatively unimpeded transport of water. Philip (1961), as have others including Portman (1958), has shown conclusively that under ideal thermal conditions, a high thermal conductivity is most desirable for the HFM from the viewpoint that sensitivity is then least affected by changes in conductivity, even if sensitivity does decrease with increasing HFM conductivity. Nevertheless, it is simple to appreciate that errors introduced by the unknown degree of thermal contact, which can be visualized as a film of low conductivity between the surroundings and the faces of the HFM, will actually diminish in importance as the HFM conductivity decreases because the thermal connection is a series one.

In view of the several conflicting properties required for optimum performance of HFM's this paper is devoted to examining the thermal performance of both uniform and nonuniform HFM's for a representative range of geometries and conductivities in two and three dimensions.

PARAMETERS DESCRIBING THE RESPONSE OF A THERMAL SENSOR

There are two ways to describe the equilibrium thermal response of a sensing body surrounded by a medium whose temperature distribution in the absence of the sensor is known. One is to state the actual change in temperature occurring in the region of the sensor, the other is to compare the

flow of heat through the sensor with that in the undisturbed medium. It is clear that this initial problem is already greatly simplified, especially in the latter case, if the undisturbed heat flow is one-dimensional. Even then, it must be recognized that the presence of a three-dimensional sensor results in three-dimensional heat flow in the region where its perturbing effect is observed. Heat or temperature sensing instruments thus fall between two extremes: one is exemplified by the exact HFM, a two-dimensional sensor oriented normal to the heat flow, the other is the exact temperature probe, a one-dimensional sensor monitoring temperature along its length.

Real HFM's respond to the mean temperature difference between the sensing surfaces of the instrument, but because of the distortion of the heat flow in general the total flux of heat through the center may be greater or less than the flux through the sensing surfaces. In his analysis, Philip (1961) has been careful to define HFM heat flow as that across the center plane, a fact that does not allow the immediate comparison of his theoretical results with most experimental data available.

If the HFM is thin enough, this problem may be neglected. And if T'_m is the mean temperature gradient across such an HFM of thermal conductivity k_m, the mean heat flux through the instrument is given by:

$$B_m \quad k_m T'_m . \tag{2}$$

A similar expression holds for the thermally undisturbed region of the surroundings:

$$B_s \quad k_s T'_s . \tag{3}$$

Under these conditions we define the temperature response of an HFM by T'_m/T'_s and the flux response by B_m/B_s. These dimensionless ratios are connected by the following expression:

$$\frac{B_m}{B_s} \quad \left(\frac{k_m}{k_s}\right)\left(\frac{T'_m}{T'_s}\right). \tag{4}$$

Clearly, the complete equilibrium thermal description of a given HFM is accomplished if either B_m/B_s or T'_m/T'_s is expressed as a function of k_m/k_s. Such a function will in general depend on the geometry of the HFM and the surroundings.

It is pertinent to inquire first as to the properties we expect of a thermally exact HFM. Consider infinitely extending surroundings in which temperature gradient, heat flux and thermal conductivity can be controlled. Recalling that an ideal HFM has $B_m = B_s$ for all values of k_m/k_s, it follows that the temperature response T'_m/T'_s of an ideal HFM must change with inverse proportionality to k_m/k_s. Figure 2 shows this characteristic and also that of the complementary type of sensor, namely the exact temperature probe. The latter must have $T'_m \quad T'_s$ for all values of k_m/k_s as shown. The alternative method of recording sensor sensitivity is shown in Figure 3. In this case B_m/B_s is shown as a function of k_m/k_s. The ideal HFM characteristic of $B_m \quad B_s$ for all values of k_m/k_s is again evident. On the other hand, the ideal temperature probe constantly indicates $T'_m \quad T'_s$, so that in this case $B_m/B_s \quad k_m/k_s$ as shown in the diagram.

Dealing, as at present, only with thermally uniform HFM's the functions connecting the dimensionless ratios T'_m/T'_s and B_m/B_s with k_m/k_s all have a common point of intersection at $k_m/k_s \quad 1$, a fact that merely indicates that at this point the HFM (or temperature probe) is thermally indistinguishable from the surroundings. The logarithmic axes display the true symmetry of the response functions. Already it should be evident that the concept of HFM conductivity k_m

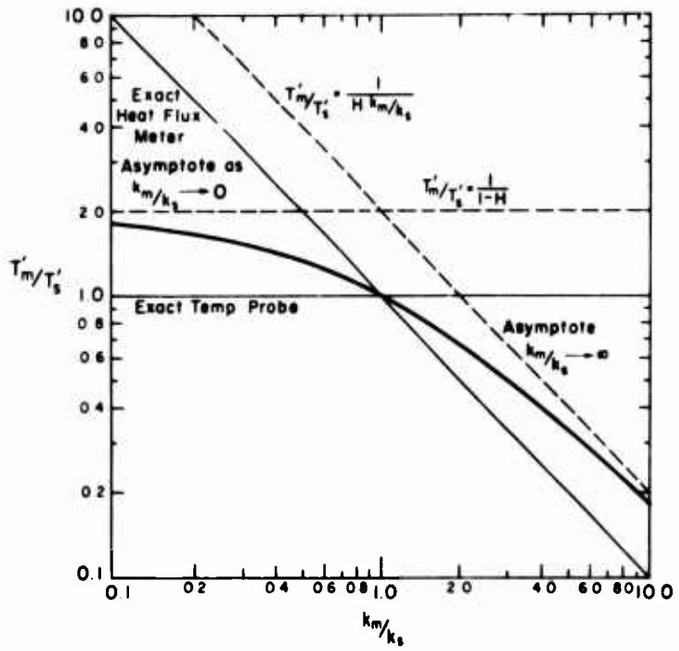

Figure 2. The dependence on conductivity ratio k_m/k_s of the sensitivity to temperature gradient of an HFM. T'_m and T'_s are the temperature gradients across the meter and the undisturbed surroundings respectively. The specific example shown is for the geometric parameter $H = 0.5$.

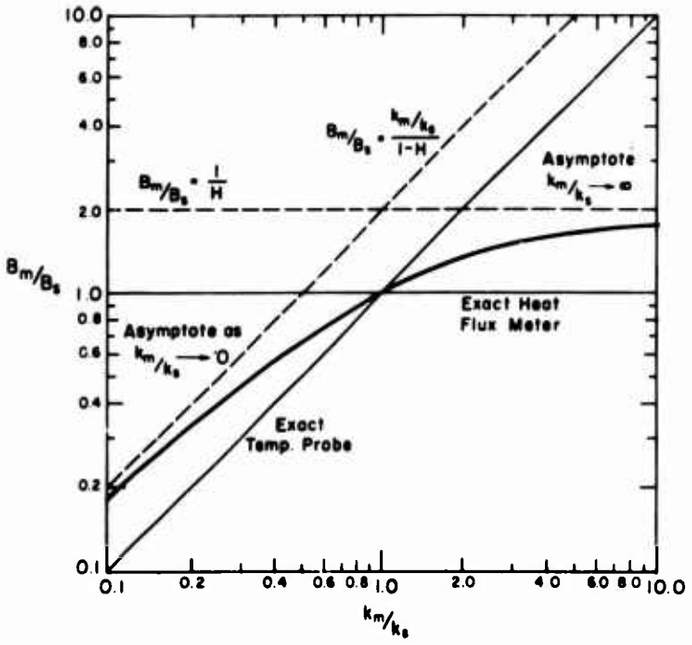

Figure 3. The dependence on conductivity ratio k_m/k_s of the sensitivity to heat flux of an HFM. B_m and B_s are the heat fluxes through the meter and the undisturbed surroundings respectively. The specific example shown is for the geometric parameter $H = 0.5$.

must be reexamined when the discussion is extended to thermally nonuniform cases. The ratio B_m/B_s can be taken to represent the "exactness" of an HFM's thermopile output if changes in the conductivity ratio k_m/k_s from unity are not taken into account.

Real thermal sensors will have a behavior with characteristics between those prescribing the performance of an ideal HFM and temperature probe in both Figure 2 and Figure 3. Portman (1958) has shown that the response functions of real HFM's can be further bounded by relatively simple considerations. As will be shown in the following section, these bounds must depend on a geometric characteristic of the HFM which Philip (1961) has calculated for the special family of cases covering ellipsoidal sensors oriented so as to display a circular cross section to the direction of undisturbed heat flow.

THERMAL RESPONSE OF A REAL HFM

The response of a real HFM is known for $k_m/k_s = 1$, when $B_m/B_s = T'_m/T'_s = 1$. The upper and lower extremes that merit discussion are the responses as $k_m/k_s \to 0$ and $k_m/k_s \to \infty$. In the initial case, we can exemplify the situation by $k_m \to 0$ and k_s remaining finite, for which $B_m \to 0$ (hence $B_m/B_s \to 0$) but T'_m/T'_s must tend to some finite value dependent on the geometry of the system. Similarly, when $k_m/k_s \to \infty$, the case $k_m \to \infty$ for finite k_s is considered; clearly $T'_m \to 0$ (hence $T'_m/T'_s \to 0$), B_m/B_s however must depend on the geometry of the system.

The above information can be summarized by writing:

$$\frac{T'_m}{T'_s} = \frac{B_m}{B_s} = 1 \quad \text{for} \quad \frac{k_m}{k_s} = 1 \tag{5}$$

$$\frac{T'_m}{T'_s} \to b \quad \text{and} \quad \frac{B_m}{B_s} \to b \cdot \frac{k_m}{k_s} \to 0 \quad \text{as} \quad \frac{k_m}{k_s} \to 0 \tag{6}$$

$$\frac{T'_m}{T'_s} \to \frac{a}{k_m/k_s} \to 0 \quad \text{and} \quad \frac{B_m}{B_s} \to a \quad \text{as} \quad \frac{k_m}{k_s} \to \infty \tag{7}$$

where a and b are functions dependent only on the geometry of the system, so that for a given HFM in infinite surroundings, a and b are both constant.

The simplest continuous functional relationship for T'_m/T'_s that obeys the constraints of eq 6 and 7 is:

$$\frac{T'_m}{T'_s} = \frac{a}{(k_m/k_s) + c_1 - 1} \tag{8}$$

where $b = a/(c_1 - 1)$. Similarly, the simplest continuous expression for B_m/B_s is:

$$\frac{B_m}{B_s} = \frac{a \cdot k_m/k_s}{(k_m/k_s) + c_2 - 1} \tag{9}$$

where $b = a/(c_1 - 1)$ from which it follows that $c_1 = c_2 = 0$. When the condition of eq 5 is applied, it follows that $c = a$ and the general HFM equations can be written:

$$\frac{T'_m}{T'_s} = \frac{1}{1 + H(k_m/k_s - 1)} \tag{10}$$

$$\frac{B_m}{B_s} = \frac{k_m/k_s}{1 + H(k_m/k_s - 1)} \tag{11}$$

where $H = 1/a$ might be termed the geometric characteristic parameter of an HFM. Equations 10 and 11, and asymptotes 6 and 7, are shown in Figures 2 and 3.

It has thus been shown that eq 11, which Philip (1961) has shown to hold exactly for a spheroidal HFM, might reasonably be expected to hold for more general shapes. It has already been pointed out that B_m is not constant throughout a real HFM, and the exact spheroidal solution is specifically restricted to the flux of heat across the center plane. In testing the general validity of eq 10 or 11, care must be taken to recognize that the flow of heat across the main sensing surfaces of an HFM may be significantly different from that across the center plane.

In the evidence which will be presented later, it will be seen that provided B_m or T_m is measured across the center plane of an HFM the support for eq 10 and 11 is good.

The parameter H can only assume values between 0 and 1. The case $H = 0$ represents the ideal temperature probe and $H = 1$ represents the ideal HFM. The set of response functions of real thermal sensors is therefore covered by the range $0 < H < 1$.

Philip (1961) found it convenient to define a dimensionless geometric ratio for HFM's given by:

$$G = \frac{\sqrt{A}}{2h} \tag{12}$$

where A is the cross-sectional area and $2h$ the thickness of an HFM. It is evident that the parameter H is partly dependent on G, but because real HFM's may be visualized as suffering from "edge effects," H is also clearly dependent on the mean distance of the surface sensing elements from the edge. This implies that an HFM of circular cross section has a higher value of H than one of square cross section having an identical value for G.

DETERMINATION OF HFM RESPONSE

Non-transient temperature distributions in a region where the temperature T and thermal conductivity k are both functions of the coordinates are described by solution of the following equation:

$$\nabla \cdot \nabla T + \frac{1}{k}(\nabla T \cdot \nabla k) = 0 \tag{13}$$

within the constraints of an appropriate set of boundary conditions.

In its simplest and one-dimensional form, eq 13 does not cover even the simplest type of HFM problem. It suffices, for example, to specify the temperatures along the length of a perfectly

insulated wire of known conductivity distribution if the temperatures at the ends of the wire are known.

In two-dimensional Cartesian coordinates, eq 13 becomes

$$\frac{\partial^2 T}{\partial x^2} + \frac{\partial^2 T}{\partial z^2} + \frac{1}{k}\left[\frac{\partial T}{\partial x} \cdot \frac{\partial k}{\partial x} + \frac{\partial T}{\partial z} \cdot \frac{\partial k}{\partial z}\right] = 0. \tag{14}$$

Since the concept of an HFM should be restricted to devices that monitor heat flow without intercepting the entire flow of heat in the surrounding medium, the two-dimensional case is the simplest one of interest. Its solution is also representative of that for a cross section of three-dimensional heat flow when identical conditions extend infinitely far in both directions normal to the cross section. For example, two-dimensional analysis would suffice to provide information on the behavior of a long bar type HFM provided the two-dimensional case represents a cross section normal to the long axis of the bar. If this bar is long enough, the unknown "edge effects" at the ends may be neglected.

The general three-dimensional case presents greater difficulty and requires solution of the following equation:

$$\frac{\partial^2 T}{\partial x^2} + \frac{\partial^2 T}{\partial y^2} + \frac{\partial^2 T}{\partial z^2} + \frac{1}{k}\left[\frac{\partial T}{\partial x} \cdot \frac{\partial k}{\partial x} + \frac{\partial T}{\partial y} \cdot \frac{\partial k}{\partial y} + \frac{\partial T}{\partial z} \cdot \frac{\partial k}{\partial z}\right] = 0. \tag{15}$$

It is clear that in general the two-dimensional case does not describe the three-dimensional cross section. Only the special case of cylindrical symmetry leads to a single solution for all plane cross sections having the central axis as a common line of intersection. For this special case with a uniform angular distribution of values for T and k about a central, z, axis, eq 13 reduces to:

$$\frac{\partial^2 T}{\partial z^2} + \frac{\partial^2 T}{\partial r^2} + \frac{1}{r}\frac{\partial T}{\partial r} + \frac{1}{k}\left[\frac{\partial T}{\partial z} \cdot \frac{\partial k}{\partial z} + \frac{\partial T}{\partial r} \cdot \frac{\partial k}{\partial r}\right] = 0 \tag{16}$$

where r, a cylindrical coordinate, represents the distance from the z axis of symmetry.

On the premise that the response of an HFM is known if the distribution of temperatures over its sensitive surfaces is known, the problem in two and three dimensions involves obtaining the solution for T, given the boundary temperatures of the surroundings and the distribution of the values for k, from eq 14 and 15 respectively.

It is well known that such solutions do not exist in general, and are available only for a limited number of special cases. In three-dimensional form, the most useful of these is that presented by Philip (1961) for a thermally uniform spheroidal HFM oriented with its circular cross section normal to the undisturbed heat flow in an infinite, also thermally uniform medium. Philip's equation is identical to eq 11.

In the present work, both electrical analogue and numerical methods were chosen to indicate basic patterns of HFM performance, accepting thermal conductivities, HFM geometry and a number of types of nonuniform HFM assemblies as variables.

ELECTRICAL ANALOGUE INVESTIGATIONS

Electrically conductive paper offers an attractive medium for observing two-dimensional conduction problems both qualitatively and quantitatively. Nickerson and Umur (1960) reported dissatisfaction with this method because of the experimental uncertainties in the conductivity of the two-dimensional simulated HFM's constructed.

In the present work, this problem was overcome by restricting the investigation to HFM's equipped with highly conductive thin cover plates and highly insulating sidewalls of various thicknesses. On the electrically conductive (or perhaps the more appropriate term would be resistive) paper highly conductive silver paint was applied with small tubular pens (such as are commonly used in precision ink drawing) to prepare accurately positioned simulated cover plates. Perfectly insulating areas were produced by cutting out with a sharp knife, a method used to simulate insulating sidewalls. By these means, the actual flow through the two-dimensional HFM was made one-dimensional so that a number of simple methods were available to vary the ratio of HFM conductivity to that of the surroundings, i.e. k_m k_s. Since the ratio and not the individual values of k_m and k_s is critical, it is unimportant which of the two is varied to produce variation in k_m/k_s. In order to generate values of k_m k_s 1, known areas of conducting paper sandwiched by the model HFM cover plates were cut. By progressively increasing the cut-out area, the whole range 0 _ k_m/k_s 1 was able to be investigated.

An initial attempt was made to produce the cases for which k_m/k_s 1 by painting in known areas of the resistive paper within and parallel to the HFM boundaries with conducting paint. But it became clear that the boundary between conducting paint and resistive paper is not a simple geometric one and the effective resistance of the paper extends for short distances beneath the paint. That is, the resistive and conductive areas couple over a finite area rather than at a distant boundary line. This fact leads to a strip of resistive paper whose active width is decreased in linear progression by the successive application of fully conducting paint to form a widening strip actually increasing in conductance at a progressively less than linear rate. The simplest valid method here would be to introduce a variable resistor to connect the two simulated cover plates.

An experimental area was defined in each case by selecting a sufficiently large piece of conducting paper. Two opposite parallel edges were given a thin strip of conducting paint to produce a constant potential along each edge when a voltage source was connected across them. A test probe consisting of a graphite pencil was electrically connected through a simple potentiometer network so as to indicate a null reading when a potential was located on the paper. In this way equipotential lines could be drawn to visualize the simulated heat flow in the vicinity of the two-dimensional HFM model. To determine relative response only the potential difference between the simulated cover plates was required to compare with the potential gradient in the undisturbed region. The area of the conducting (or resistive) sheet was regarded as being large enough if the presence of the simulated HFM caused no significant change in current flow between the two fixed potential boundaries.

The results of the first type of investigation are shown in Figure 4. This is for a set of rectangular HFM's equipped with thin, conducting, sensitive surfaces and thin insulating sidewalls. The responses shown as a function of k_m/k_s are relative to the case k_m/k_s 1 in each instance. The presence of walls and cover surfaces causes the actual response for the cases k_m/k_s 1 to be a little different from unity. While it is evident that the thicker the cover plates the greater the discrepancy would be, later measurements showed that increasing the thickness of the insulating sidewalls had even more pronounced effects on the response. For either type of variation, it is clear that the concept of HFM conductivity k_m requires reexamination. In this first set of cases, k_m was regarded as being the conductivity of the homogeneous HFM material located within the

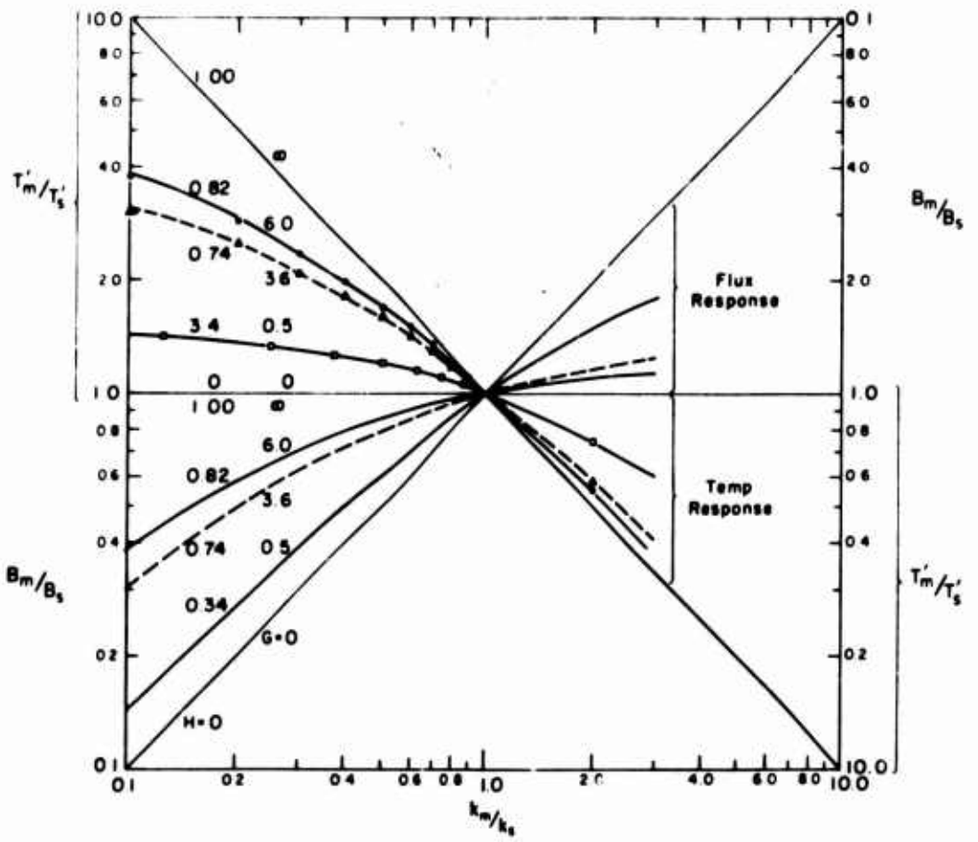

Figure 4. The results of two-dimensional electrical analogue measurements are shown by experimental points, each sequence being for a definite geometric ratio G. The lines joining these points are given by eq 10 and 11 with the values of the geometric parameter H chosen to fit.

confines of the highly conducting and insulating boundaries. Ideally, both of these types of boundary should be infinitesimally thin.

As seen in Figure 4, the results are as expected from the discussion developed in the section on thermal response. For each geometric ratio G, which in the two-dimensional case is not defined by eq 12 but as the ratio of the length of the HFM's cross section to its thickness, a distinct value of H, the HFM geometric parameter, was calculated. The curve connecting the experimental points for each case is of the form prescribed by eq 10 with a mean value for H calculated to give the best fit. It is clear that there is no ambiguity about fitting these curves as the experimental agreement with eq 10 is excellent and no dependence of H on the value of k_m/k_s can be detected.

These cases are simple because the presence of insulating sidewalls means that the flux through such HFM's is the same for all planes in the HFM parallel to the covers. There is thus no difficulty in determining the appropriate value of T'_m or B_m at the center of the HFM, even for small values of G, the geometric ratio.

Since the relative thicknesses of both the insulating sidewalls and the conducting covers are very small compared to that of the sensitive portion of the HFM, their presence does not significantly affect the mean value of the thermal conductivity of the composite body in the direction of the heat

flow. On the other hand, the effective conductivity in the plane of the HFM is significantly increased by a conducting thin cover. Unfortunately no extensive analogue comparisons of HFM's with and without covers were made, mainly because representative sampling in the coverless case is relatively difficult. It can be argued, however, that the presence of even a thin but highly conductive cover causes the HFM response to be shifted toward that of the ideal, because the HFM boundary becomes isothermal, leading to a reduced distortion of the undisturbed heat flow pattern in the vicinity of the HFM. Indeed, as will be seen in a later section, numerically computed values of the parameter H for HFM's without covers were significantly below those calculated from the analogue data for covered HFM's of identical geometric ratio.

ANALOGUE INVESTIGATION OF WALLED OR "FOCUSING" HFM'S

When the thickness of the insulating sidewalls is increased in the plane of an HFM, the flow of heat is significantly modified by the presence of the insulators as well as by the sensitive portion of the HFM. Since the latter is often a thermopile or in any case a sensor sensitive to a temperature difference across it, the term thermopile will be used as a convenient label, even for the two-dimensional cases presently under discussion.

Analogue measurements show that an insulating wall or edge always increases the temperature response of a thermopile and that this effect increases monotonically with the extent of the insulator, being more pronounced for lower values of k_m, the thermopile conductivity.

Figure 5 shows the electrically simulated isotherms and lines of heat flow for a set of cases based on one two-dimensional thermopile of geometric ratio equal to 3.6. The simple cases in Figures 5a and 5b represent uniform HFM's of infinite and zero conductivity. Extensive sidewalls are shown in Figure 5c for the high extreme of thermopile conductivity. It is clear that in the latter case the flow of heat is actually focused into the thermopile, and accordingly HFM's which employ this phenomenon might well be referred to as being of the focusing type.

A real point of difficulty arises in deciding on the nature of the parameters chosen to describe the behavior of these instruments which are an example of symmetrical nonuniform HFM's. The insulating wall confers one analytical advantage only, in that all heat flowing through the HFM actually passes through the thermopile alone, thus obviating the analytical difficulty caused by a varying flux through different planes as discussed previously.

In the analogue technique adopted, perfectly insulating regions were created simply by cutting out the appropriate area of conducting paper. Figure 6 shows the results on HFM response of increasing the wall thickness which transversely sandwiches a two-dimensional thermopile whose geometric ratio otherwise remains constant at 3.6. Although it is interesting to speculate that the addition of highly conductive (rather than insulating) walls would decrease (rather than increase) the overall response in a similar manner, the real advantage may be recognized in the useful degree, as well as control, of response magnification. This thermal amplification is obtained without any physical change to the thermopile itself. It implies that for a given value of k_m/k_s and a single thermopile, within limits, the sensitivity desired can be achieved by suitable choice of the insulating wall thickness.

When the response is plotted as a function of k_m/k_s, as in the simple cases of uniform HFM's, the definition of k_m is chosen to remain as the actual value of the thermopile conductivity, since the calculation of a mean HFM conductivity incorporating the depressing effect of the low conductivity insulator leads only to confusion. In Figure 7, the HFM response has been shown both for temperature difference T'_m/T'_s and for heat flux B_m/B_s. Because these ratios are not equal to 1 when $k_m/k_s = 1$ except for an insulating wall of infinitesimal thickness, normalized values are shown, which are derived from the relation:

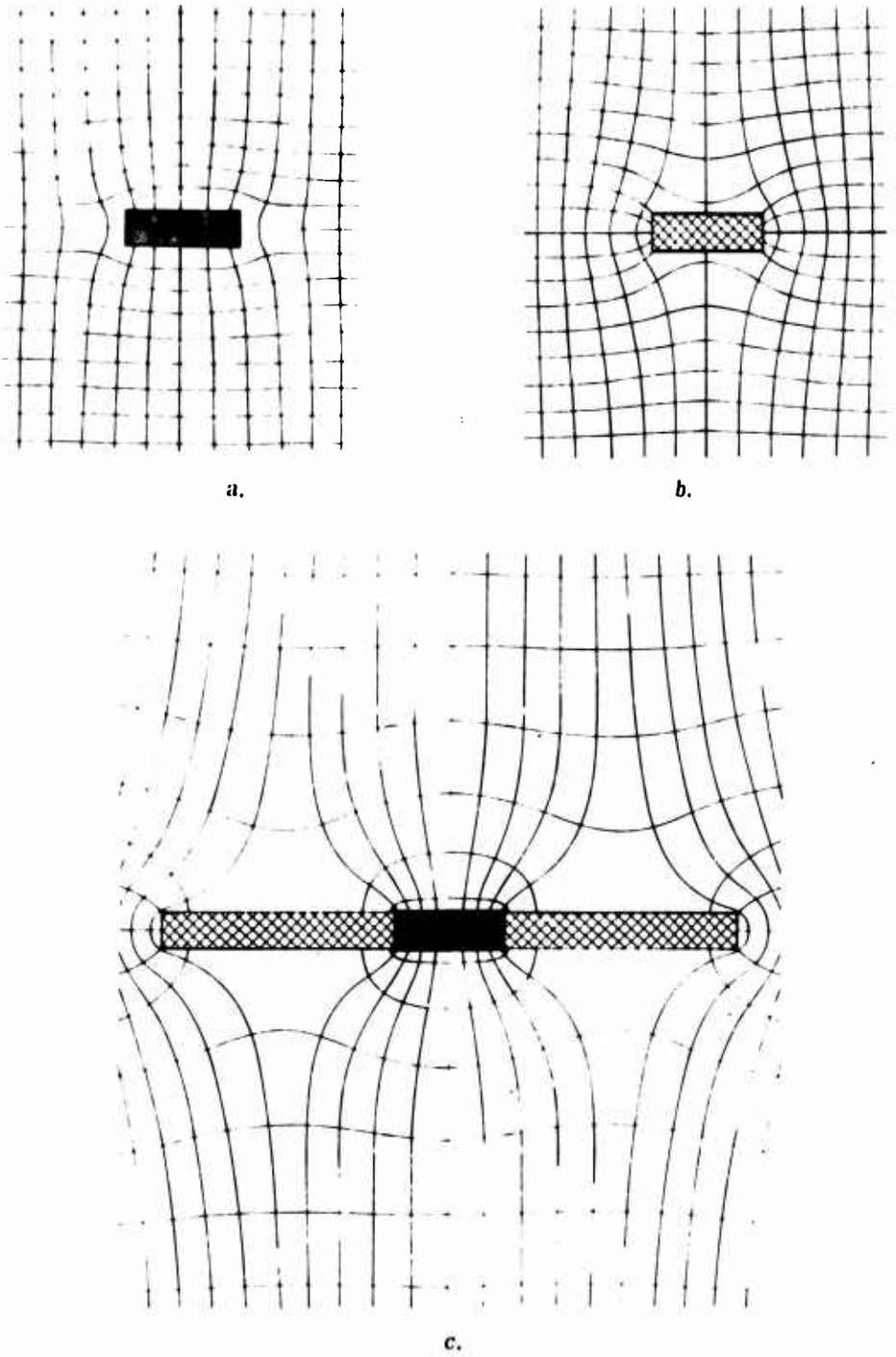

Figure 5. Simulated isotherms and lines of heat flow are shown by analogue measurements for a two-dimensional HFM (uniform except for conducting covers) for the extreme cases of a) infinite and b) zero conductivity ratio. In c), the focusing effect of insulating edges is clearly seen.

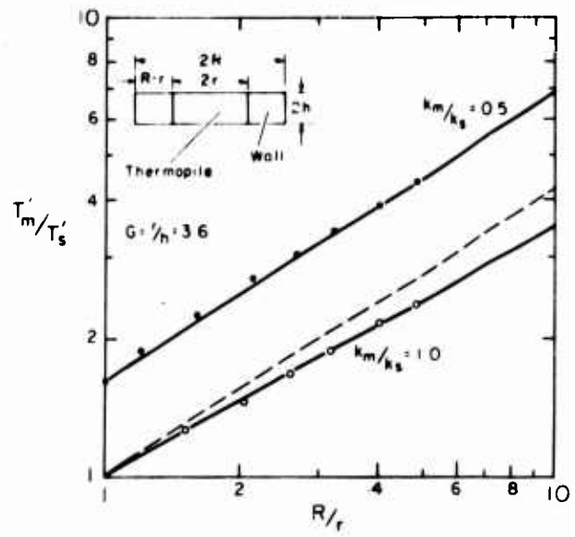

Figure 6. The effect on the response of a thermopile caused by the addition of insulating walls at the edges, resulting in a nonuniform, "focusing" HFM. The measurements shown were obtained by electrical analogue analysis.

$$\left(\frac{T'_m}{T'_s}\right)_N = \frac{(T'_m/T'_s)}{(T'_m/T'_s)_{k_m/k_s}} \tag{17}$$

with a similar expression defining the normalized flux response. Figure 7 shows normalized, as well as actual, temperature and flux responses for a given thermopile equipped with three different wall thicknesses, one of which is zero.

A most important property of the normalized response functions is that they are seen to be accurately described by eq 10 and 11 with appropriate values of the parameter H, which can be determined for each case. So closely do the theoretical values agree with the observed points that the solid lines are in fact given by eq 10 and 11 with values of H selected to give best fit in the mid-range. The apparent disagreement which develops in the region $k_m/k_s = 0.1$ is never greater than 5% and is almost certainly due to the decreased accuracy of the analogue determination since extreme values of k_m/k_s lead to a change in the total conduction across the experimental plane in which the HFM lies.

Whereas a uniform two-dimensional HFM located in infinitely extending surroundings can be specified completely by the geometric ratio G and the conductivity ratio k_m/k_s, even the simple nonuniform HFM's described above require the additional ratio R/r, where $2R$ is the overall transverse dimension of the HFM whose thermopile has a width $2r$. Zero wall thickness therefore implies R/r 1. If the insulating wall has an appreciable conductivity the HFM response practically defies a general graphical representation.

Even in the present instance, where the insulating wall is specified to have a fixed zero conductivity it is unrealistic to aim at complete representation covering all possible combinations. What is important is that the normalized responses have been shown to obey eq 10 and 11 which indicates that even in more complex cases of walled HFM's, a single geometric parameter, H, can

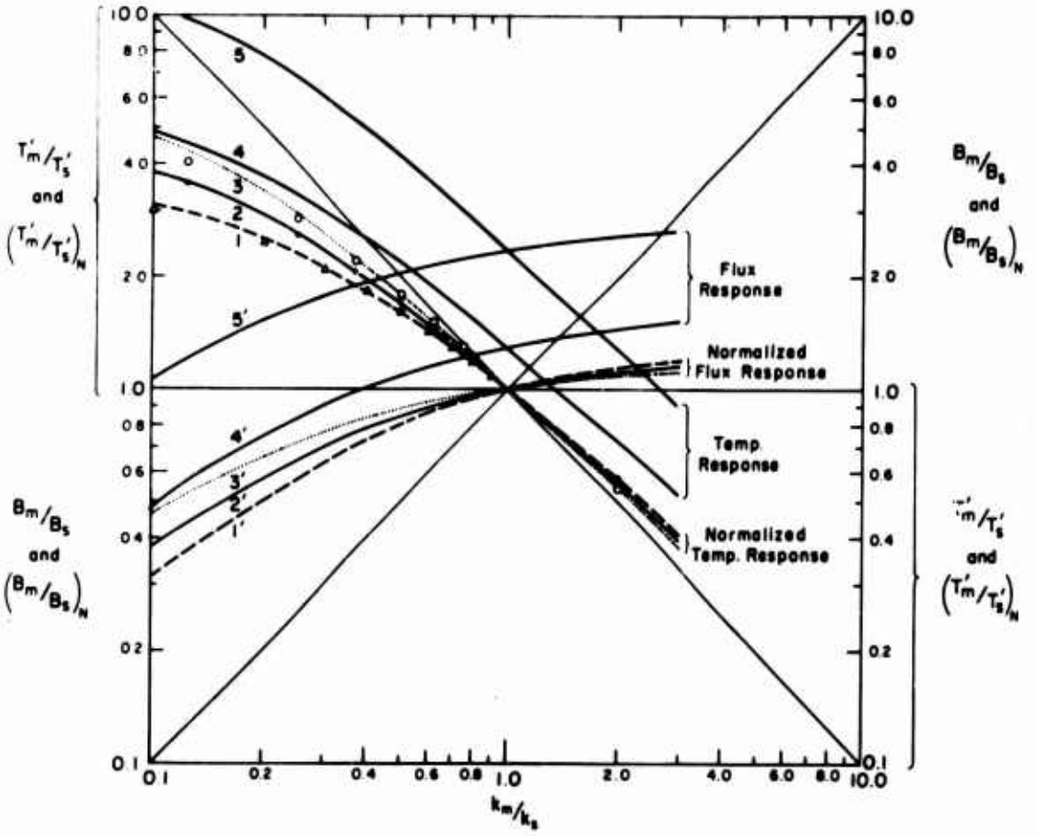

Figure 7. Two-dimensional analogue measurements of the responses of edge-insulated (or walled) HFM's. The method of experimental observation results in the points being normalized to the case where $k_m/k_s = 1$. Results are shown in the form of normalized temperature response 1, 2, and 3 which are for HFM's for which the values of R/r are respectively 1.00, 1.65, and 5.00. Curves 1, 4 and 5 show the actual ratio between temperature gradients in the thermopile and the surrounding medium. The curves 1', 2', 3', 4' and 5' are the corresponding sensitivities expressed as heat flux ratios. Equation 10 prescribes curves 1, 2 and 3 when H is 0.75, 0.82 and 0.88 respectively. The location of curves 4 and 5 follows from the information in Figure 6.

be determined by calibration for one known value of k_m/k_s and the reference case $k_m = k_s$. In the simpler case of a uniform HFM the latter case is trivial and known. The value of H thus determined then suffices for numerical calculation of the normalized responses for any value of k_m/k_s, from eq 10 and 11, with an accuracy which appears to lie within the limits of the present experimentation.

NUMERICAL ANALYSIS OF TWO- AND THREE-DIMENSIONAL UNIFORM AND EDGE-INSULATED HFM'S

Numerical methods provide an alternative means to analogue studies of two-dimensional HFM's. The chief advantage of numerical computation lies in the capacity to solve more difficult three-dimensional cases. The analysis was restricted to two-dimensional and cylindrical cases, for which

a representative two-dimensional cross section could be obtained for the solution. The method chosen was simply to replace eq 14 and 16 by finite difference approximations and to solve these new equations by what was essentially a relaxation method on a DDP-24 computer. This computer limited the number of elements in the x-z field to about 1600 each for the temperature T and conductivities k. This limited field capacity meant that this computer was not well suited to analyze cases where the HFM had an extreme geometric ratio G. In fact the best results were expected to occur for the region $0.5 < G < 2$. Another effect was to restrict the useful computations to cases for which the conductivity ratio k_m/k_s was not too far removed from unity. Just what constituted "too far" in both of these types of restriction was tested by solving the numerical approximations to eq 14 and 16 twice in each case. Each repeated computation involved a finite difference approximation for first derivatives approaching from the opposite direction. When the solutions became sensitive to the direction of approximation and differed excessively, they were rejected. This explains why the data obtained for the responses pertain only to HFM's for which, approximately, $0.25 < G < 4.0$ and $0.2 < k_m/k_s < 5.0$. Although these limitations are a little unfortunate, the acceptable results nevertheless encompass the most interesting and definitive regions of HFM behavior.

The first set of two- and three-dimensional HFM's studied had simple rectangular shapes or cross sections respectively. The results for the two-dimensional cases (Fig. 8) are expressed as temperature responses and indicate incomplete agreement with eq 10. Examination of Figure 5 shows that when $k_m < k_s$, the heat flux through the meter is greater at the boundaries intercepting the undisturbed heat flow than at the center. When $k_m > k_s$, the opposite is true. However, in order to conform to the conditions set by Philip (1961) for the spheroidal HFM solution, B_m in both two- and three-dimensional cases must be the heat flux across the center. Since HFM's with thermopiles respond to the temperature difference across the whole sensor, this corresponds to a dependence on the mean heat flux $\bar{B}_m$. If the heat flux across the boundary is given by B_{mb}, it follows that:

$$\left.\begin{aligned} B_{mb} > \bar{B}_m > B_m \quad & \text{if } k_m < k_s \\ B_{mb} = \bar{B}_m = B_m \quad & \text{if } k_m = k_s \\ B_{mb} < \bar{B}_m < B_m \quad & \text{if } k_m > k_s . \end{aligned}\right\} \tag{18}$$

If the geometric parameter H is calculated from eq 11 using values of $\bar{B}_m$, it follows from eq 18 that

$$H(k_m < k_s) < H(k_m > k_s) \tag{19}$$

instead of the equality which holds for the spheroidal case. Examination of the original numerical data shows that if B_m rather than $\bar{B}_m$ is calculated and used as a basis for determining H, dependence on k_m/k_s is reduced to the extent of being hidden within experimental accuracy. Although this may be theoretically satisfying, it still leaves the geometric parameter H, as determined by thermopile output, with an undesirable conductivity dependence.

Although this effect might be expected to decrease as the geometric ratio G increases, the use of edge insulating walls is suggested in order to keep the heat flux through an HFM constant. Because a constant value of H successfully described the analogue responses of two-dimensional HFM's equipped even with extensive insulating walls, in Figure 7, the responses of HFM's having walls of low but realistic rather than zero conductivities were also computed. In these numerical experiments, the conductivity of the edge walls was kept at one-tenth of that of either the thermopile k_m or the surroundings k_s, depending on which was least. Since the numerical field was limited in size, it

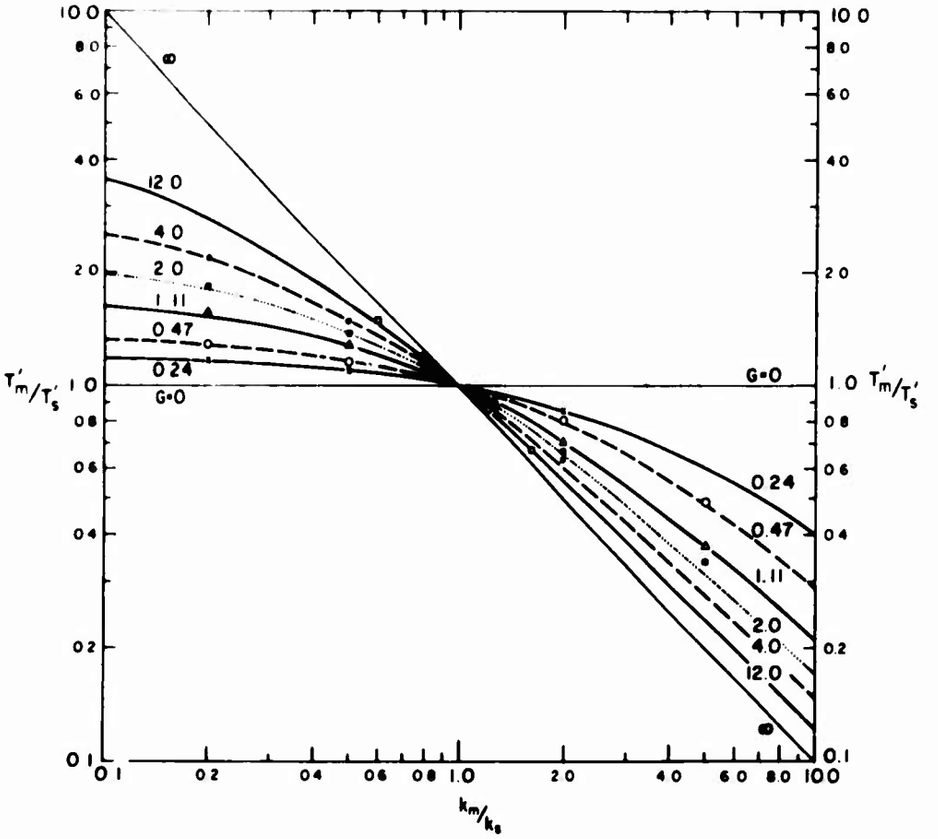

Figure 8. Numerically computed points are shown for the responses of a number of uniform HFM's whose geometric ratios G are shown. The curves drawn through these points have been generated by eq 10 with values of H chosen to provide the best fit. The points for the case G = 12 have been calculated from the data of Nickerson and Umur (1960).

was not possible to keep the ratio of wall thickness to thermopile width constant as the geometric ratio was varied. As the results summarized in the next section show, the geometric parameter tended to become less dependent on k_m/k_s when the insulating walls were kept thin. With thicker walls a significant fraction of the flux of heat, which varies as the ratio k_m/k_s changes, becomes neglected. It is probable that in order to secure significant constancy of the parameter H in eq 11 a high quality insulating material must be used in practice.

THE HFM GEOMETRIC PARAMETER AS A FUNCTION OF THE GEOMETRIC RATIO

The geometric parameter H is shown as a function of the geometric ratio G in Figures 9, 10 and 11. Figure 9 shows the results obtained by analogue analysis for HFM's with thin, perfectly insulating walls and conducting covers. Each of the three points shown represents a value of H calculated from the experimental data shown in Figure 4, for the range $0.25 \leq k_m \leq 4.0$. The nature of the curve joining the three points will be discussed shortly. Figure 10a shows the numerically determined results for uniform two-dimensional rectangular HFM's. Although the points show a significant dependence of H on k_m/k_s, some of this is caused by computing errors inherent in the

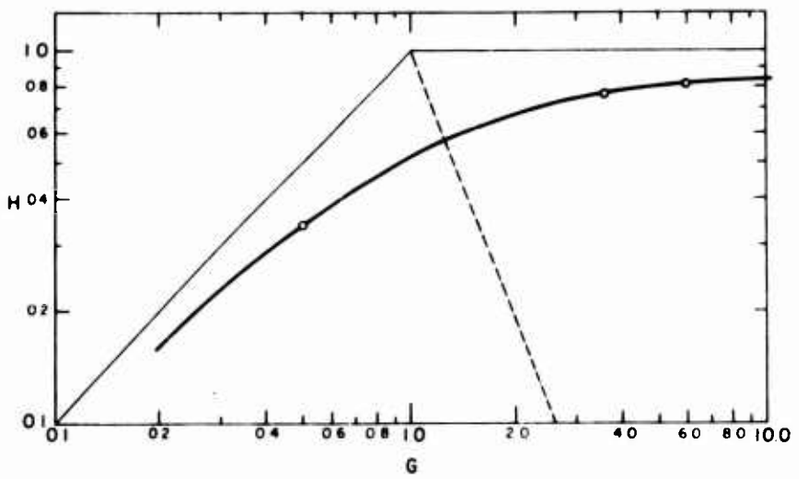

Figure 9. The geometric parameter H as determined for a two-dimensional HFM with conducting covers by analogue analysis, as a function of the geometric ratio G.

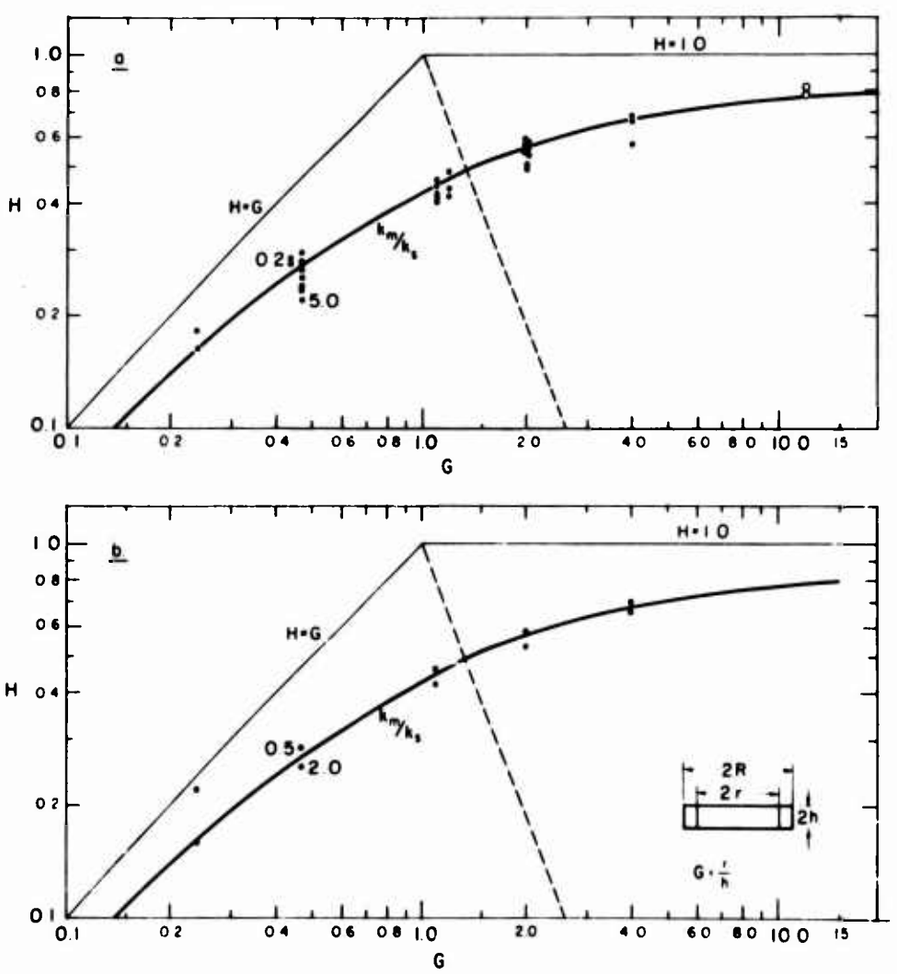

Figure 10. The geometric parameter H as a function of geometric ratio G determined a) for uniform and b) for edge-insulated two-dimensional HFM's.

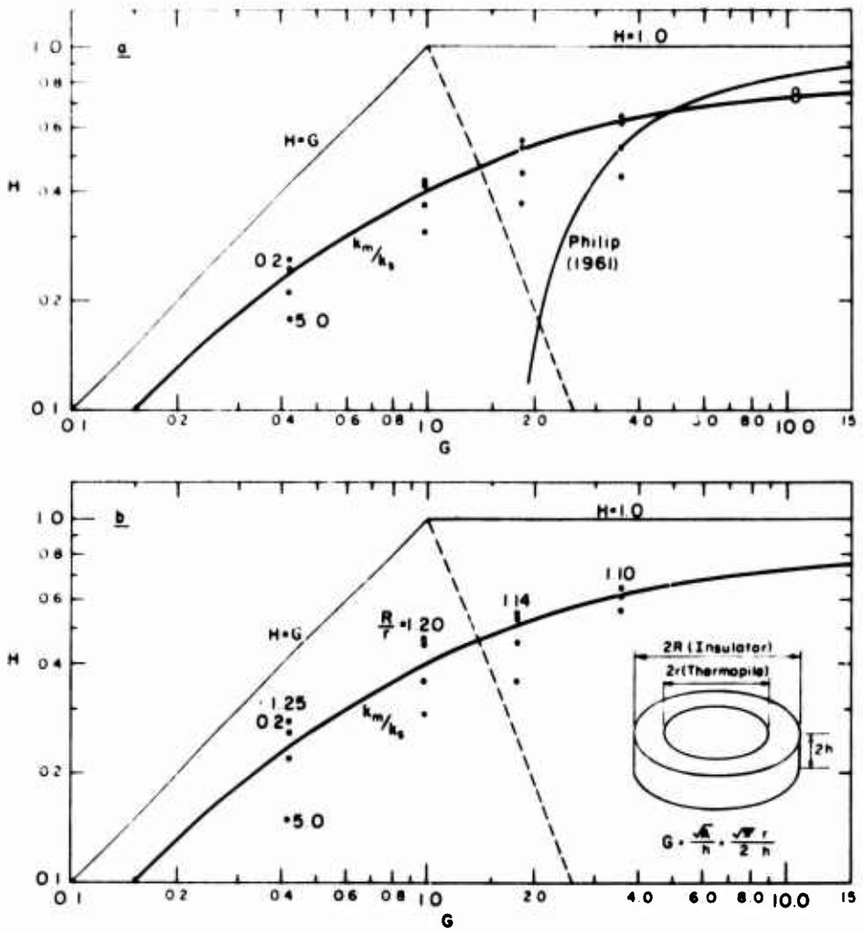

Figure 11. The geometric parameter H as a function of geometric ratio G determined a) for uniform and b) for edge-insulated three-dimensional cylindrical HFM's.

use of a small numerical field. The case of two-dimensional HFM's with insulating edge walls is summarized by the data in Figure 10b. The connecting curve drawn is identical to that in Figure 10a. The errors introduced by neglecting the flux through the thicker, only finitely insulating walls, is clearly seen as G decreases. Otherwise, the change is minimal, mainly because computing errors mask the improvement for higher values of G for which a more marked reduction in the amplitude of H would be expected. The difference between the analogue and numerical results is of the right sign in view of the different conditions represented. Those two values calculated from the independently computed data of Nickerson and Umur (1960) and shown as open circles (o) fit into the scheme of Figure 10a satisfactorily.

The three-dimensional cylindrical cases are similarly summarized by Figures 11a and 11b, which show the results for uniform and edge-insulated HFM's respectively. Again the two points shown as open circles in Figure 11a are values recalculated from data presented by Nickerson and Umur (1960). It is seen that H is greater for a two-dimensional rectangular HFM than for a cylindrical meter of identical cross section or even one of identical geometric ratio. This is to be expected because the overall proximity of the HFM edge in relation to the main body of the sensor is greater in the three-dimensional case.

The two-dimensional result also holds in the case of a long, right-angled bow-shaped HFM in three dimensions. Here the two-dimensional solution can be regarded as a typical cross section,

since if the bar is long enough, the edge effects at distant ends contribute negligibly in modifying the total response. For example, a bar-shaped HFM monitoring vertical heat flow and having a vertical and two horizontal relative dimensions of 1, 10 and 100 respectively would have a three-dimensional geometric ratio of 31.6. However, for a two-dimensional, perpendicular, vertical cross section this ratio would be equal to 10, a fact emphasizing the need to discriminate between two- and three-dimensional values of G, say G_2 and G_3. The value of H 0.76, read from Figure 10 for G_2 10, should also hold for the bar type HFM since the major dimension is long enough for end effects to be negligible. Using the three-dimensional description for the same bar, incaution results in a value of H = 0.83 being assigned when no discrimination is made with regard to HFM shape.

It can be argued that this is to be expected since for a given geometric ratio a cylindrical thermopile has its thermojunctions situated further from the edge than a long, thin, rectangular cross section. Indeed it is likely that the circular cylindrical HFM provides the greatest value of H which can be achieved by any three-dimensional shape with a given value of G. For this reason, Philip's (1961) argument, which leads to constancy of the geometric parameter H for all regularly shaped HFM's having an equal geometric ratio G, probably leads to serious inaccuracies even when HFM's with circular and square cross sections are compared. Philip's equation for sufficiently large values of G is:

$$H = 1 - \frac{1.70}{G}. \tag{20}$$

All of the H-G diagrams in Figures 8, 9 and 10 show a smooth curve, indicating a definite functional connection. The nature of these curves was deduced from the accurately known relationships between H and G, *viz*:

$$H \to 1 \text{ as } G \to \infty$$

$$H \to 0 \text{ as } G \to 0.$$

If the latter tendency is replaced by:

$$H \to G \text{ as } G \to 0$$

then the basis for choosing the asymptotes becomes:

$$\log H \to 0 \text{ as } \log G \to \infty$$

$$\log H \to \log G \text{ as } \log G \to -\infty.$$

On the logarithmic diagram, the points appear to be symmetrically distributed about the dashed line shown bisecting the angle between the asymptotes in each case, so that the simplest continuous function having these properties is a hyperbola. The hyperbolas shown as the connecting curves in the figures can be shown to be given by:

$$(\log H)^2 - \log G \cdot \log H = (\log H_0)^2 \tag{21}$$

where H_0 is the value of H when $G = 1$, i.e. $\log G = 0$. Only half of the hyperbolas are required and it follows that

$$\log H = \frac{1}{2}\left[\log G - \sqrt{(\log G)^2 - 4(\log H_0)^2}\right]. \tag{22}$$

Table I. The geometric HFM parameter H as a function of the geometric ratio G for a number of values of $H(G = 1)$, i.e. H_0.

$H_0 \backslash G$	*0.10*	*0.20*	*0.30*	*0.40*	*0.50*	*0.60*	*0.80*	*1.0*	*2.0*	*3.0*	*4.0*	*5.0*	*6.0*	*8.0*	*10.00*	*20.00*	*30.00*	*40.00*	*50.00*	*60.00*	*80.00*	*100.00*
0.37	0.07	0.12	0.17	0.21	0.25	0.28	0.33	0.37	0.49	0.56	0.60	0.62	0.64	0.67	0.69	0.74	0.76	0.78	0.79	0.80	0.81	0.82
.38	.07	.13	.18	.22	.25	.28	.34	.38	.51	.57	.61	.64	.66	.68	.70	.75	.77	.79	.80	.80	.82	.83
.39	.07	.13	.18	.22	.26	.29	.35	.39	.52	.58	.62	.65	.67	.70	.71	.76	.78	.80	.81	.81	.82	.83
.40	.07	.13	.18	.23	.27	.30	.36	.40	.53	.60	.63	.66	.68	.71	.73	.77	.79	.81	.82	.82	.83	.84
.41	.07	.13	.19	.23	.27	.31	.36	.41	.54	.61	.65	.67	.69	.72	.74	.78	.80	.82	.82	.83	.84	.85
.42	.07	.14	.19	.24	.28	.31	.37	.42	.56	.62	.66	.68	.70	.73	.75	.79	.81	.82	.83	.84	.85	.86
.43	.08	.14	.19	.24	.28	.32	.38	.43	.57	.63	.67	.70	.72	.74	.76	.80	.82	.83	.84	.85	.85	.86
.44	.08	.14	.20	.25	.29	.33	.39	.44	.58	.65	.68	.71	.73	.75	.77	.81	.83	.84	.85	.85	.86	.87
.45	.08	.14	.20	.25	.30	.33	.40	.45	.59	.66	.69	.72	.74	.76	.78	.82	.84	.85	.85	.86	.87	.87
.46	.08	.15	.21	.26	.30	.34	.41	.46	.60	.67	.71	.73	.75	.77	.79	.83	.84	.85	.86	.87	.87	.88
.47	.08	.15	.21	.26	.31	.35	.42	.47	.62	.68	.72	.74	.76	.78	.80	.84	.85	.86	.87	.87	.88	.89
.48	.08	.15	.21	.27	.31	.36	.43	.48	.63	.69	.73	.75	.77	.79	.81	.84	.86	.87	.88	.88	.89	.89
.49	.08	.15	.22	.27	.32	.36	.43	.49	.64	.70	.74	.76	.78	.80	.82	.85	.87	.88	.88	.89	.89	.90
.50	.08	.15	.22	.28	.33	.37	.44	.50	.65	.72	.75	.77	.79	.81	.82	.86	.87	.88	.89	.89	.90	.91
.51	.08	.16	.22	.28	.33	.38	.45	.51	.66	.73	.76	.78	.80	.82	.83	.87	.88	.89	.89	.90	.90	.91
.52	.08	.16	.23	.29	.34	.38	.46	.52	.67	.74	.78	.80	.81	.83	.84	.88	.89	.90	.90	.90	.91	.92
.53	.08	.16	.23	.29	.34	.39	.47	.53	.68	.75	.79	.81	.82	.84	.85	.89	.89	.90	.91	.91	.92	.92

It is seen that eq 22 provides a reasonable interpolation for the data points shown in Figures 8, 9 and 10. The fit for the less scattered analogue data is particularly good.

On the logarithmic scale shown, some extrapolation is justified and Table I shows values of H calculated from eq 22 as a function of G for a number of values of H_0. This has been done because H_0 varies for different HFM shapes. The values of H for high values of G are generally not as high as would be expected from Philip's (1961) work (eq 20) but until further, more precise computations have been made using a larger numerical field, all that can be concluded is that eq 22 is of a more satisfactory form than eq 20 especially for lower values of G. Furthermore, eq 22 is applicable to temperature probes as well and shows the transition of responsive properties between the two extreme types of thermal sensors.

THE DETERMINATION OF THERMAL CONDUCTIVITY BY HFM PAIRS

Even if the geometric parameter of an HFM has been determined, the relative response remains unknown unless the conductivity ratio is known. Because the conductivity of the HFM surroundings may change substantially during a period of observation, the conductivity ratio must be found at the same time that a heat flow measurement is made if the heat flux through the surroundings B_s is to be computed from the measured heat flux through the HFM B_m.

Conductivity changes of surroundings may be encountered during the course of a single set of observations such as when dry soil is wetted by rain, snow compacts or the temperature of sea ice changes. Soil conductivities may lie in the range 0.8×10^{-3} to 8×10^{-3} cal cm^{-1} sec^{-1} °C^{-1} (de Vries, 1952). Within the density and temperature ranges 0.3 to 0.92 g cm^{-3} to 60° C respectively Weller and Schwerdtfeger (1970) have shown the thermal conductivity of snow and ice to be from 0.6×10^{-3} to 7.4×10^{-3} cal cm^{-1} sec^{-1} °C^{-1}. The conductivity of sea ice is between $3 \cdot 10^{-3}$ and 5×10^{-3} cal cm^{-1} sec^{-1} °C^{-1} (Schwerdtfeger, 1963). The geometric mean of thermal conductivities encountered in these typical terrestrial surface materials is of the order of $2 \cdot 10^{-3}$ cal cm^{-1} sec^{-1} °C^{-1}, which within a factor of $5^{\pm 1}$ includes almost all solid substances commonly encountered to any extent near the earth's surface. It seems realistic to design any one set of HFM measurements to encompass a conductivity ratio changing by up to a factor of $5^{\pm 1/2}$, i.e. a total span of 5.

The simplest method of monitoring these changes appears to be by employing pairs of thermal sensors and observing the change in the ratio of the two normalized flux responses, the latter being defined by eq 11. If the conductivity ratio k_m/k_s is now written as η_1 and η_2 for the two different HFM's having geometric parameters H_1 and H_2 respectively, then the relative flux response ratio may be written:

$$R = \frac{1 - H_2(1 - \eta_2)}{1 - H_1(1 - \eta_1)} \frac{\eta_1}{\eta_2}. \tag{23}$$

If the two HFM's are installed in mutually non-disturbing yet sufficiently close and similar locations, then the ratio $\eta_1/\eta_2 = a$ may be expected to remain constant and it is convenient to write $\eta_1 = \eta$ and $\eta_2 = a\eta$ so that:

$$R = \frac{1 - H_2(1 - a\eta)}{1 - H_1(1 - \eta)} \cdot \frac{1}{a}. \tag{24}$$

The sensitivity of this ratio to conductivity change is given by:

$$\frac{dR}{d\eta} = \frac{aH_2(1 - H_1) - H_1(1 - H_2)}{a[1 - H_1(1 - \eta)]^2}. \tag{25}$$

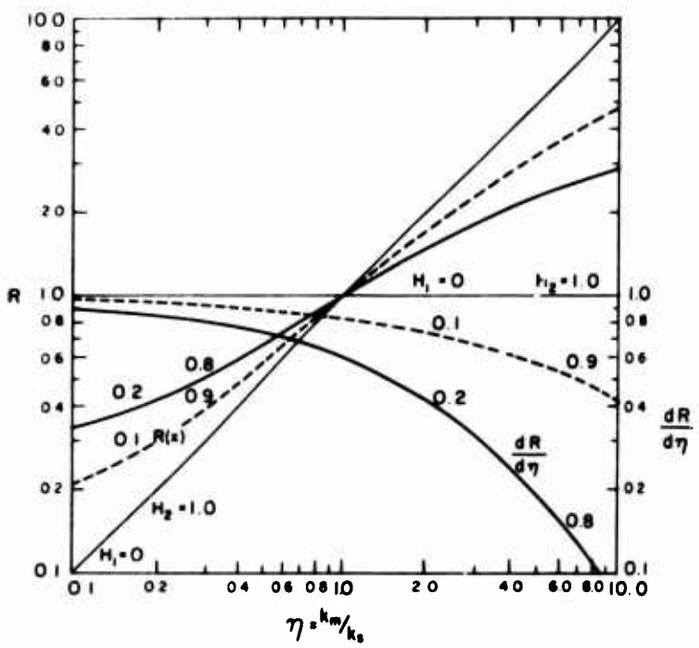

Figure 12. The ratio of the normalized flux responses R for pairs of HFM's whose geometric parameters are respectively 0.9 and 0.1, and 0.8 and 0.2. The sensitivity of R to change in the conductivity ratio η is given by $dR/d\eta$.

It is evident that the sensitivity is greatest when H_2 is as large and H_1 as small as possible with $a > 1$. Furthermore, it follows under these conditions, since $0 < H < 1$, that $dR/d\eta$ becomes negligibly dependent on a. There is therefore no advantage gained by not having $\eta_1 = \eta_2$ or $a = 1$, for which:

$$R = \frac{1 - H_2(1 - \eta)}{1 - H_1(1 - \eta)} \tag{26}$$

and

$$\frac{dR}{d\eta} = \frac{H_2 - H_1}{[1 - H_1(1 - \eta)]^2}. \tag{27}$$

The above equations represent the results obtained with a pair of HFM's having equal conductivities but different geometric parameters. This conveniently allows the use of a given thermopile material worked either into two different shapes or with completely different thicknesses of insulating edge walls.

From eq 26 and 27 it is seen that

$$R \to \frac{1 - H_2}{1 - H_1} \text{ as } \eta \to 0$$

and

$$R \to \frac{H_2}{H_1} \text{ as } \eta \to \infty.$$

The sensitivity $dR/d\eta$ is always less than 1 and monotonically tends to zero as $\eta \to \infty$.

Figure 12 shows the response ratio R and its sensitivity to conductivity change $dR/d\eta$ as a function of the conductivity ratio $k_m/k_s = \eta$ for three different pairs of sensors. It is clear that the greatest sensitivity is obtained when $(H_2 - H_1)$ is large, a factor that becomes particularly important when $\eta > 1$, a region for which most HFM's would be designed. The almost trivial conclusion is that the ideal conductivity sensing pair is the exact HFM and the exact temperature probe.

Allison (1968) has had some success in monitoring conductivity changes in soil by the use of HFM pairs. The sensitivity, unfortunately, was impaired by the use of meters whose geometric parameters were not different enough.

SENSITIVITY OF HFM'S TO LOCATION

There are several possibilities arising in the location of HFM's which may result in a significant alteration in the sensitivity (relative to that when $k_m = k_s$, i.e. $\eta = 1$) established for the ideal reference condition of infinitely extending surroundings. These are most easily discussed by considering distances along axial directions, referred to an HFM, where a specified degree of perturbation in the temperatures of the surrounding material is observed.

When the numerically computed temperature fields are examined, it becomes apparent that distances X_n and Z_n, measured along X and Z axes having their origin at the HFM centroid, can be defined, where n is the positive or negative percentage change in the undisturbed temperature caused by the introduction of the HFM. If the half width and half thickness of the meter (or its cross section in the three-dimensional case) are given by r and h respectively, then convenient dimensionless indications of the HFM's disturbance are defined by the ratios X_n/r and Z_n/h. The two- and three-dimensional geometric ratios G are given by r/h and $(\sqrt{\pi}/2)(r/h)$ respectively.

For HFM's having a geometric ratio $G > 1$, numerical analysis shows that the disturbed temperature patterns for both two-dimensional rectangular and three-dimensional cylindrical HFM's having the same geometric ratio (including two- and three-dimensional geometric ratios) are not significantly different when the axial distances of 10% temperature disturbance, X_{10} and Z_{10}, are computed. Figure 13 shows X_{10}/r and Z_{10}/h as a function of $\eta = k_m/k_s$ with a degree of accuracy which does not discriminate between the two- and three-dimensional HFM's discussed. Although complete symmetry does not appear to exist between the cases $\eta = k_m/k_s$ and $1/\eta$, the differences in the corresponding values of X_n and Z_n are not large and are covered by the error bars shown in the figure. This means that the values of X_{10}, say, shown for $\eta = 4$, for example, are also the appropriate values for $\eta = 1/4$.

For the range $2 < n < 20$, the following very approximate relationship holds:

$$\frac{X_n}{X_{3n}} \approx \frac{Z_n}{Z_{3n}} \approx 2.$$

As an example, the values of X_3/r and Z_3/h have been shown on a separate scale in Figure 13. From the discussion of HFM properties on p. 6-7, X_n and Z_n would be expected to tend to some constant value as η, $1/\eta \to \infty$, depending on n and the meter geometry.

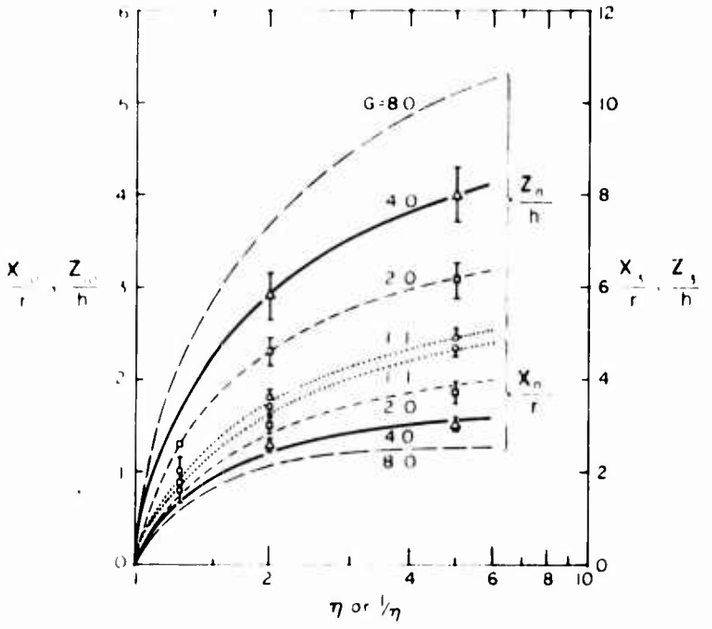

Figure 13. The axially measured distances X_n and Z_n from an HFM centroid, where these coincide with points at which the perturbation caused by the HFM on the undisturbed temperature of the surrounding material is n%. The case where n = 10 has been computed numerically for geometric ratios 1.1, 2.0, and 4.0 with an estimation for G = 8.0 shown. The scale for n = 3 is an approximation.

These values are accurate enough to allow planning for the spacing of pairs or groups of HFM's in such arrays so as to ensure minimal interference.

An important factor influencing HFM sensitivity is the proximity of a boundary of the surrounding material. Most frequently this boundary will be the terrestrial surface. Referring to Figure 13 it is seen, to take an example, that for an HFM having a geometric ratio $G = 4$ and a thickness of 0.5 cm, i.e. h 0.25 cm, if k_m/k_s $\eta = 3$, then $Z_3/h = 6$ and $Z_5 = 1.5$. This implies that only that portion of the temperature field which would be modified less than 3% by the presence of this particular HFM would be cut off if installed with its center at a depth of 4 cm below the surface. Because only one side of the HFM is affected, the error in the HFM reading calibrated for infinite surroundings is certainly less than half of 3%.

Unfortunately, micrometeorology demands the value of the conducted flux of heat at the earth's surface, rather than a few centimeters below. It is apparent that the error in an HFM calibration might now be more serious. Philip (1961) has discussed this case, stressing the need for some assumption with regard to the temperature distribution at the terrestrial surface. In the absence of an HFM, the surface temperature may be regarded as isothermal, but with an HFM at or just below the surface, it would remain so only if k_m/k_s $\eta = 1$. With heat flow occurring outwards from the ground, surface temperature would be decreased if $k_m < k_s$ and increased if $k_m > k_s$. With heat flow originating from an above-ground source, much depends on whether the heating is localized, such as by absorption of radiation, or continuously distributed as occurs during the presence of a strong wind near the ground. With strong ventilation, ground surface temperature differences would be diminished. If ground temperatures remain unchanged by any above-ground process, it can be

argued that the HFM tends to conduct a flux of heat equal to that of the surroundings, because if $k_m < k_s$, T'_m increases, and if $k_m > k_s$, T'_m decreases when an HFM is installed near the ground surface, rather than at depth.

There are thus two extreme cases when an HFM is located at the surface of the ground. Either the surface temperature remains uniform, or the heat flux does. The real situation will lie somewhere in between and almost certainly defy precise description.

The constant heat flux extreme is trivial in that $B_m = B_s$ and no HFM correction at all is involved. The uniform surface temperature extreme is more interesting. Because of the isotherm which exists along the horizontal center line or plane of HFM's in infinite surroundings, a fact that can be seen in Figure 5, an HFM installed at the surface would have the same temperature distribution beneath it as one of twice the thickness located at depth. This is equivalent to stating that an HFM of geometric ratio G at the surface has a relative sensitivity lying between unity and that holding for an HFM with a geometric ratio of $2G$ located in infinitely extending surroundings.

The perhaps surprising conclusion is that the relative sensitivity of an HFM in an infinite medium actually lies within the range bounded by the two extremes just described. It follows that in the absence of knowledge of conditions above the surface, it is most reasonable to regard HFM sensitivity as being unchanged by the nearby boundary above. At night, with less atmospheric mixing occurring above the ground surface, the calibration will tend to the uniform flux condition. During the day, with more turbulent exchange occurring horizontally, the uniform temperature condition will tend to apply.

EXPERIMENTAL HFM CALIBRATION TECHNIQUES

In the previous sections it has been demonstrated that for precise work, all types of HFM should be calibrated as a function of the conductivity ratio. To do this experimentally is both difficult and time consuming as the response must be observed for a representative number of different conductivity ratios which can only be achieved by repeating observations with a number of different surrounding materials whose conductivity and temperature gradient are known.

A more economical alternative is to determine the geometric parameter H by a lesser number of measurements. The relative sensitivities shown in Figure 14 which are based on eq 10 and 11 can then be read off for the appropriate value of H.

Thermally uniform HFM's are the simplest to deal with and an estimate of the appropriate value of H may be obtained for the appropriate value of the geometric ratio in Table I. Greater precision would be attained by obtaining just one measurement of the sensitivity for $k_m \neq k_s$ after the actual value of k_m has been determined. For uniform meters the relative response for $k_m = k_s$ is known to be unity and therefore requires no separate determination.

Two items of equipment were constructed to simplify the calibration measurements. The first consisted simply of two stirred chambers of water controlled at different temperatures with apertures cut to permit turbulent contact with the entire sensitive area of the thermopile surfaces, as shown in Figure 15. With this simple device, the actual response of an HFM to a given temperature difference across it could be observed. Furthermore, the linearity of this response, as well as temperature dependence, were easily determined. If the thickness of an HFM under test is given by $2h$, then the temperature gradient across the meter is given by

$$T'_m = \frac{T_a - T_b}{2h} \tag{28}$$

where T_a and T_b are the temperatures of the stirred enclosures of water.

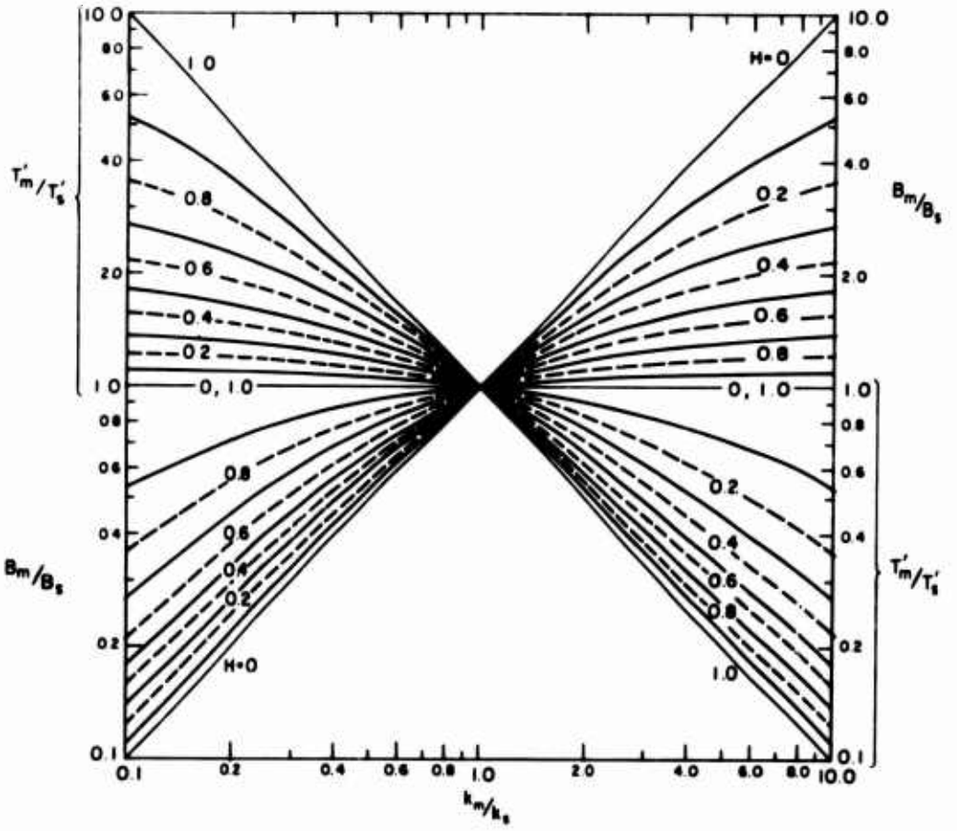

Figure 14. Normalized temperature and flux responses shown as a function of geometric parameter and conductivity ratio as calculated from eq 10 and 11.

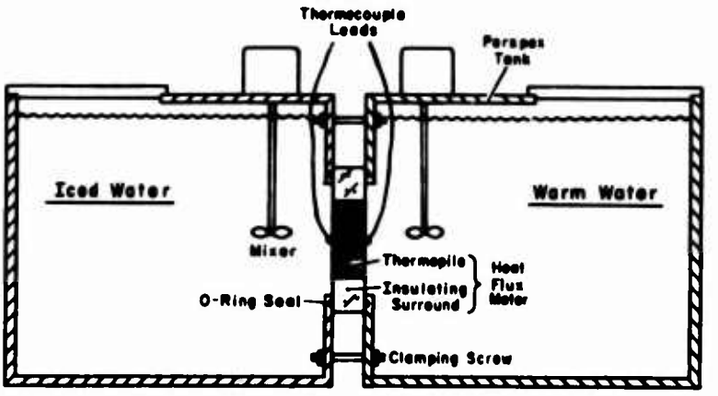

Figure 15. Tanks used to establish the output from a thermopile in response to a temperature difference maintained across it by means of stirred water at controlled temperatures.

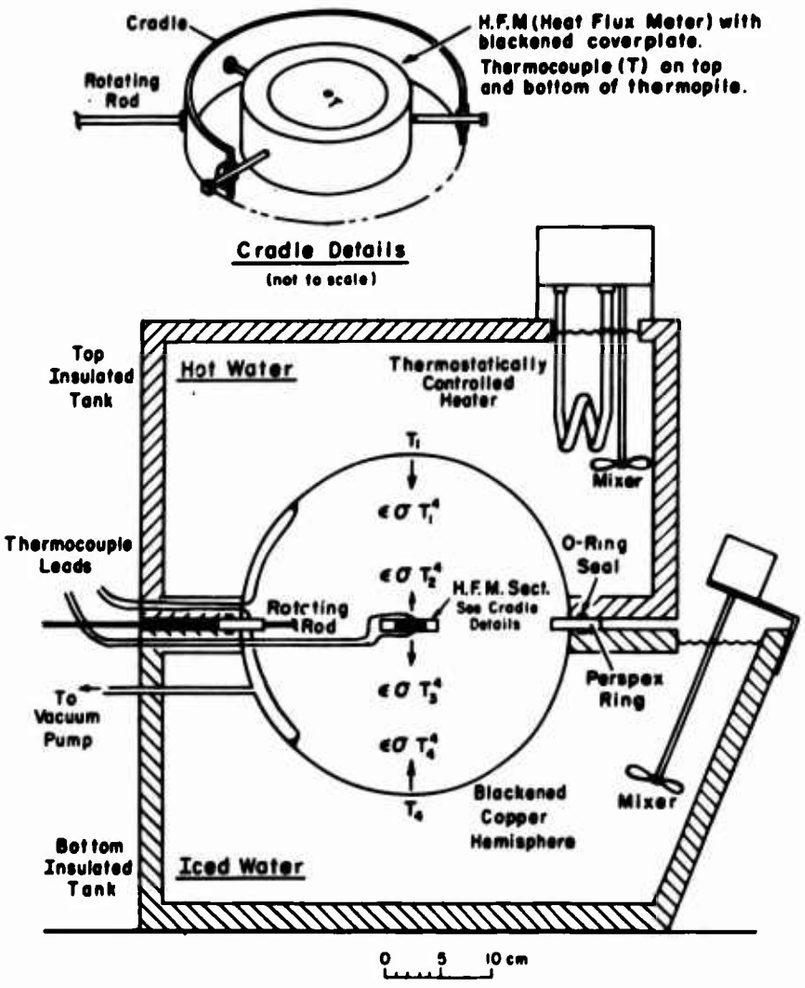

Figure 16. Radiation enclosure used to establish the output from a thermopile in response to a calculable flux of heat resulting from a known radiation balance.

The second calibrative device was designed to allow a known flux of conducted heat to pass through the HFM. As pointed out in the first section, if the thermal conductivity of an HFM is not well known it is difficult to prepare purely conductive surroundings so as to ensure an undisturbed flow of heat, even through HFM's without edge insulation. Accordingly the infrared radiation enclosure shown diagrammatically in Figure 16 was constructed. The HFM under test was coated with a black paint of known emissivity. The similarly blackened radiating hemispheres were kept at known temperatures by the stirring of thermostatically controlled water in the surrounding jackets. Finally, in order to ensure that all heat transferred to and from the thermopile surfaces was by radiation alone, the volume enclosing the meter under test was evacuated. Referring to Figure 16 it is seen that the equilibrium heat balance of the HFM reduces to an equation connecting conducted and radiated heat fluxes as follows:

$$B_m = \epsilon\sigma[\epsilon(T_1^4 - T_4^4) + T_3^4 - T_2^4]. \tag{29}$$

provided that ϵ is not too much less than 1, so that multiple reflections can be considered negligible.

The temperatures T_1, T_2, T_3 and T_4 are easily measured and ϵ and σ, the emissivity of the applied paint and the value of the Stefan-Boltzmann constant respectively, are known.

The output of an HFM thermopile can thus be measured for a known heat flux B_m, and by changing the temperatures of the water jackets linearity and temperature coefficient can be established. The temperatures of the HFM thermopile surfaces, T_2 and T_3, were monitored by small thermocouples carefully soldered to the aluminum cover plates, a process easily accomplished by using a sharp soldering iron beneath a coating of paraffin wax.

It is thus possible to determine that temperature gradient T_m and heat flux B_m associated with an equal thermopile output. Under these conditions, $(T_a - T_b) = (T_3 - T_2)$ and

$$B_m = k_m T_m \tag{30}$$

and it follows from eq 28 and 29 that

$$k_m = \frac{2h\epsilon\sigma|(T_1^4 - T_4^4) + T_3^4 - T_2^4|}{(T_3 - T_2)}. \tag{31}$$

Equation 31 implies that k_m could be determined by a single set of observations taken in the radiation enclosure. In practice, however, since $(T_3 - T_2)$ is usually small, this factor is determined with greater accuracy by observations using greater temperature differences in the temperature gradient equipment described earlier.

Nonuniform, including edge-insulated, HFM's require an additional, that is two, test measurements in conductive surroundings for calibration. In one of these, k_m should be different from k_s as before; in the other, k_m should be equal or close to k_s in value. This additional measurement allows the determination or estimation by interpolation of the actual relative responses for $k_m = k_s$ and thus, as outlined on p. 11-13, of the normalized relative responses. Conductive tests which have been described by Schwerdtfeger and Weller (1967) were carried out with ice and snow in insulated cylindrical containers whose dimensions complied with the requirements discussed in the previous section.

The results for the thermopile whose flux responses were summarized in Figure 1 will be taken as an example in Table II.

Table II. Experimental determination of geometric parameter H for an HFM.

Temperature gradient sensitivity	17.5 mV/°C cm^{-1}	
Heat flux sensitivity (as radiometer)	7.5 mV/mcal cm^{-2} sec^{-1}	
Thermal conductivity of thermopile, k_m	2.3 mcal cm^{-1} °C^{-1} sec^{-1}	
Test surroundings	**Ice**	**Snow**
Conductivity of surroundings, k_s (units as for k_m)	5.0	2.0
Conductivity ratio, k_m/k_s	0.46 ± 0.03	1.15 ± 0.10
Relative flux response observed	1.20	1.67
Relative flux response when $k_m = k_s$	1.60	
Normalized relative flux response	0.75 ± 0.02	1.04 ± 0.02
Geometric parameter, H	0.72 ± 0.06	0.71 ± 0.3

It is useful to note that this experimental technique which allows the determination of the thermal conductivity of a thermopile can be used with disk-shaped samples of any material.

It is important to establish the accuracy of the determination of H. If the notation k_m/k_s η and $(B_m B_s)_N$ β is used, then from eq 11:

$$H \quad \frac{1 - \eta/\beta}{1 \quad \eta}. \tag{32}$$

After partial differentiation, it follows that if $\Lambda\eta$ and $\Lambda\beta$ are the magnitudes of the uncertainties in η and β respectively, the uncertainty in H is given approximately by:

$$\Lambda H \quad \frac{\eta}{\beta^2} \cdot \frac{1}{(1 \quad \eta)} \cdot \Lambda\beta + \frac{1}{\beta} \cdot \frac{(1 \quad \beta)}{(1 - \eta)^2} \cdot \Lambda\eta. \tag{33}$$

Equation 33 was used to calculate the uncertainties shown for H in Table II. The closeness of the agreement between the two determinations is rather fortuitous and for a satisfactory determination of H, the conductivity ratio η k_m/k_s must be chosen to be as different from unity as possible. Even the more acceptable determination with ice as surroundings for the HFM barely fits these criteria.

In many circumstances involving uniform HFM's, in view of the difficulty of establishing the geometric parameter with any degree of precision, it may prove preferable simply to consult Table I which gives theoretically determined values of H as a function of the geometric ratio. The operational description of such an HFM is then completed by a determination of its conductivity k_m by the experimental method discussed earlier.

HFM DESIGN CRITERIA

The most frequent requirement of an HFM is that its response should change as little as possible in a given experimental location even though the conductivity of the surrounding medium may be altered. Rewriting eq 11 with the notation of the previous section:

$$\beta - \frac{\eta}{1 + H(\eta - 1)} \tag{33}$$

which on differentiation yields:

$$\frac{d\beta}{d\eta} \quad \frac{1 - H}{[1 + H(\eta - 1)]^2} \tag{34}$$

From the latter equation, it is evident that the requirements demand as small a value for $d\beta/d\eta$ as possible. This is achieved if the geometric parameter H (and hence the geometric ratio G) as well as the conductivity ratio η are made as large as possible. Such meters have been described by Deacon (1950) and Hatfield and Wilkins (1950).

In practice, however, experimental locations often deviate far from the thermally ideal conditions envisaged in the simple specification above. When the state of the surroundings is not conducive to good thermal contact with HFM surfaces, Philip (1961) has shown that by viewing the thermal resistance as formed by a thin layer of air, the actual and usually unknown modification caused to an HFM's effective sensitivity leads to completely unacceptable results which err by up to 55% for the terrestrial range of conductivities cited on p. 21. Philip's data show that under these conditions greater error arises in the use of higher conductivity HFM's. It follows, therefore, that the design conductivity of an HFM should lead to a value of k_m/k_s just high enough to ensure a value above unity for the range of conductivities expected for the surroundings.

In granular surroundings such as dry soil, sand, and snow, poor thermal contact will arise from the inability of individual grains to fit their faces to the HFM surfaces as extensively as to neighboring grains. Under such conditions, thermal contacts can be greatly enhanced by the presence of a suitably thick film of silicone grease through which the smooth, rigid HFM surfaces can couple thermally to the irregular boundaries of the surroundings.

In sufficiently moist soils, thermal contact does not constitute a problem but the high cross section of an HFM preventing the natural diffusion of water must be considered. The simplest action is to maintain a high conductive cross section but allow the passage of water (and vapor) through holes drilled through the HFM. If the mean thermal conductivity of the thermopile material is significantly different from the intended surroundings, the HFM holes would have to be filled with a compensating substance during calibration. This is one more reason to design for a conductivity ratio not too far removed from unity.

A further difficulty arises in translucent media such as ice and snow. In this situation it is best to paint the thermopile surfaces white to minimize heating by light absorption, even though the upper nearby surroundings are perturbed by increased light and a volume remains shaded below. The relative importance of this disturbing effect is reduced when the focusing HFM used by Schwerdtfeger and Weller (1967) is used. This instrument, which employs a thermopile surrounded by a transparent insulator, results in a sensor of increased conductive cross section while keeping the radiative cross section unchanged when compared to the original thermopile.

Serious difficulties arise when an HFM is required to register transient heat flows. Ideally, a meter for this purpose should be uniform in all directions and have the same conductivity and heat capacity per unit volume as the surrounding material. If the meter is thin enough, a probably satisfactory compromise is to keep the sensor heat capacity as low as possible, aiming for a high thermal diffusivity, so that the transmission of temperature waves is not impeded.

Inevitably, each experimental situation will have to be assessed and the choice of a relatively simple HFM whose sensitivity in location can be reliably assessed from unambiguous geometric and conductive data will have to be weighed against a more complex nonuniform HFM whose characteristics can only be established with precision by a series of experimental observations.

LITERATURE CITED

Allison, I.F. (1968) Non-uniform heat flux meters. Unpublished M.Sc. thesis, University of Melbourne.

Deacon, E.L. (1950) The measurement and recording of the heat flux into the soil. *Quarterly Journal of the Royal Meteorological Society*, vol. 76, p. 479-483.

DeVries, D.A. (1952) The thermal conductivity of granular materials. *Bulletin of the International Institute of Refrigeration*, Annexe 1952-1, p. 115-131.

Hatfield, H.S. and Wilkins, F.J. (1950) A new heat-flow meter. *Journal of Scientific Instruments*, vol. 27, p. 1-3.

Ho, P.; Schwerdtfeger, P. and Weller, G. (1968) The energy exchange within a vegetation layer. *Archiv für Meteorologie, Geophisik und Bioklimatologie*, Ser. B. 16, p. 262-271.

Nickerson, R.J.; Choi, N.Y. and Marcus, S. (1959) Methods and equipments for measuring soil temperature and heat flow through the soil. U.S. Army Signal Research and Development Laboratories, Fort Monmouth New Jersey, Contract DA-36-039 SC-78174.

Nickerson, R.J. and Umur, A. (1960) An analysis of methods and equipments for measuring heat flow through the soil. U.S. Army Signal Research and Development Laboratories, Fort Monmouth New Jersey, Contract DA-36-039 SC-78174.

LITERATURE CITED (Cont'd)

Philip, J.R. (1961) The theory of heat flux meters. *Journal of Geophysical Research*, vol. 66, no. 2, p. 571-579.

Portman, D.J. (1958) Conductivity and length relationships in heat-flow transducer performance. *Transactions American Geophysical Union*, vol. 39, no. 6, p. 1089-1094.

Schwerdtfeger, P. (1963) The thermal properties of sea ice. *Journal of Glaciology*, vol. 4, no. 36, p. 789-807.

_____ and Weller, G. (1967) The measurement of radiative and conductive heat transfer in ice and snow. *Archiv für Meteorologie, Geophisik und Bioklimatologie*, Ser. B. 15, Heft 1-2, p. 24-38.

Weller, G. and Schwerdtfeger, P. (1970) Thermal properties and heat transfer processes of the snow of the central Antarctic plateau. *Proceedings of ISAGE*, International Association for Scientific Hydrology, Publication No. 86.

DOCUMENT CONTROL DATA - R & D

(Security classification of title, body of abstract and indexing annotation must be entered when the overall report is classified)

1. ORIGINATING ACTIVITY (Corporate author)
U. S. Army Cold Regions Research and Engineering Laboratory
Hanover, New Hampshire 03755

2a. REPORT SECURITY CLASSIFICATION
Unclassified

2b. GROUP

3. REPORT TITLE
THE MEASUREMENT OF HEAT FLOW IN THE GROUND AND THE THEORY OF HEAT FLUX METERS

4. DESCRIPTIVE NOTES (Type of report and inclusive dates)

5. AUTHOR(S) (First name, middle initial, last name)
Peter Schwerdtfeger

6. REPORT DATE
November 1970

7a. TOTAL NO. OF PAGES
37

7b. NO. OF REFS
12

8a. CONTRACT OR GRANT NO.

8b. ORIGINATOR'S REPORT NUMBER(S)
Technical Report 232

b. PROJECT NO.

c. DA Task 4A062112A89401

9b. OTHER REPORT NO(S) (Any other numbers that may be assigned this report)

d.

10. DISTRIBUTION STATEMENT
This document has been approved for public release and sale; its distribution is unlimited.

11. SUPPLEMENTARY NOTES

12. SPONSORING MILITARY ACTIVITY
U. S. Army Cold Regions Research and Engineering Laboratory
Hanover, New Hampshire 03755

13. ABSTRACT

The behavior of heat flux meters has been examined by experimental, electrical analogue and numerical means. The results indicate the more general applicability of the flux meter equation first proposed by Philip (1961) for the special case of spheroidal meters, provided certain precautions are taken. The purely geometric parameter appearing in this equation has been related to meter shape and a functional connection has been suggested. It is proposed that pairs of thermal sensors be used to monitor thermal conductivity continuously and the use of nonuniform "focusing" heat flux meters is recommended in cases where the physical cross section of a thermopile should remain small compared to the resultant thermal cross section. Finally a number of calibration techniques are reported, including the use of a novel radiation enclosure in which meters are temporarily tested as net radiometers.

14. Key words:
Analogies
Calibrating
Heat flow meters
Heat flux
Heat transfer
Micrometeorology
Thermal measuring instruments

DD FORM 1 NOV 68 1473 REPLACES DD FORM 1473, 1 JAN 64, WHICH IS OBSOLETE FOR ARMY USE.